Linear Response Polarizability Tensor Theory for Vibrational Circular Dichroism: VCD and IR Absorption Bandshape Calculations of α-Helical and β-Sheet Polypeptides

Hirotoshi ITO* and Y. J. I'HAYA
Department of Applied Physics and Chemistry, The University of Electro-Communications, 1-5-1 Chofugaoka, Chofu, Tokyo 182

(Received November 5, 1993)

Based upon a fixed partial charge approximation of Schellman, we present a linear response polarizability theory for the bandshapes of vibrational circular dichroism (VCD) and vibrational absorption spectra of biopolymers, where a polymer vibrational polarizability tensor is derived from monomer polarizability tensors in terms of Green's operator method within a dipole–dipole approximation. The new formalism can be easily programmed by utilizing a quite similar algorithm appearing in the polarizability theory regarding electronic CD, which was previously presented. However, the theoretical framework is shown to be essentially the same as that in the excitonic treatment of the secular matrix equation method of Snir, Frankel, and Schellman, and that of their version prescribed by Diem and co-workers as an extended coupled oscillator model. Using the experimental data of the monomer transition moments of the amide I and II bands, the VCD and IR absorption bandshapes were computed for α-helical and β-sheet polypeptides. The computed VCD bandshapes were found to well predict the conformations of polypeptides. We also discuss whether an allowance is necessary or not for multistate interband mixings between constituent monomers in VCD calculations, since it is generally believed that the characteristic bands of constituent monomers can be used as localized probes to detect the conformations of biopolymers, if one follows the assumption of Schellman and co-workers that there are no interband interactions between different levels.

Before vibrational circular dichroism (VCD) became capable of distinguishing secondary structures in solution-phase and solid-phase (film) proteins by using specific spectra of the amide residue,[1—4] several theories concerning VCD bands for small molecules and polypeptides were presented in the 1970's.[5—7] These theories have provided a theoretical background for developing VCD experimental studies. Especially before the advent of experimentally available VCD spectrometers, the VCD spectra of the amide I and II bands for α-helical and β-sheet polypeptides were first theoretically predicted by Snir et al.[7] by using a coupled oscillator approximation between the same single levels of different residues; their calculations have thus been a guide to the various VCD studies of biopolymers. It has been revealed along with this work that the VCD spectra measured for biopolymers can provide good ground-state properties and geometrical information concerning the solution and solid phases,[1—4] if we properly choose characteristic and finger-print vibrations of their chromophores. This knowledge, that the characteristic bands can be used as localized probes to observe the conformations of biopolymers, is of course based upon such an assumption that a characteristic band of a certain residue interacts with the same characteristic bands of the different residues, but may not drastically interfere with any other bands. The separate use of the amide I and II vibrations has been such a good example. However, in this paper, not only single-state interband coupling, but also multi-state interband couplings, are formally taken into account.

Soon after Snir et al.,[7] calculations of the infrared absorption bandshape spectra (IR) for the amide I vibration of antiparallel and parallel β-sheet polypeptides were carried out by Chirgadze and Nevskaya[8,9] using the resonance interaction exciton theory of the transition dipoles, which can be related with the fixed partial charge (FPC) model of Schellman et al.[6,7] Their resonance interaction theory,[8,9] in which a normal coordinate analysis is unnecessary, has been shown to give a realistic prediction of the IR absorption bandshapes.

For the VCD bands of DNA molecules, Gulotta et al.[10] and Zhong et al.[11] have re-described the Snir–Frankel–Schellman scheme by a recipe called an extended coupled oscillator (ECO) approximation. This version takes into account only vibrationally excitonic coupling interactions between certain specific single levels of monomer units in a polymer. Namely, a single-state interband excitonic mixing only is also involved in the ECO approximation. Furthermore, the ECO approximation has been applied to calculations of small linear oligopeptides in order to determine their conformation, so as to fit the observed rotational as well as dipole strengths and the dipolar splitting.[12] Also, in the ECO approximation VCD calculations of a small cylic oligopeptide have been shown to qualitatively predict the VCD of the amide I band, which has been calculated for the torsion angles (ϕ,ψ) determined from X-ray and NMR data.[13] For large polypeptides, Birke et al.[14] have applied the ECO method to an analysis of the VCD spectra of a random-coil poly(L-tyrosine) to find its suitable conformations in terms of the backbone torsion angles (ϕ,ψ). However so far, these VCD approximations have not been sufficiently capable of predicting all of the features of the VCD bandshapes. For example, regarding the observed monosignate bands, most

of VCD calculations inadequately yield bisignate bandshapes, which are oftern called conservative bands. Besides, most of VCD models require an artificial introduction of the bandshape functions. As a small step towards a sufficiently good vibrational exciton approach, we present a VCD formulation which is capable of naturally introducing bandshape functions by making use of Green's operator method.

First, we assume a model Hamiltonian for biopolymers within the FPC-like coupled oscillator approximation of Schellman.[6] Then, based on the non-interacting part of this Hamiltonian, we derive the monomer vibrational polarizability tensors, from which we can construct the polymer polarizability tensor by taking into account the dipole-dipole interactions. Once, the polymer polarizability tensor is obtained, we can readily derive the VCD and IR absorption bandshape functions, since the theoretical structure for the VCD is quite similar to the Fano-DeVoe type coupled oscillator model for the electronic CD and electronic absorption spectra.[15] In the present paper we do not allow for excited electronic contributions to the IR and VCD bandshapes. Namely, we do not take into account the mixings of some electronic excited states with the ground electronic state due to vibronic couplings.[16,17] For checking the present theory, VCD calculations were carried out for the well-known structures of polypeptides determined by the dihedral torsion angles of the polypeptide backbone (ϕ,ψ) without considering any side-chain effects.

Vibronically Excitonic Model Hamiltonian for Biopolymer

Let us represent the total ground vibronic state of a polymer (N-mer) as follows:

$$|e_0v_0^0> \equiv |\prod_n^N \psi_{0n}(\mathbf{q},\mathbf{Q})\phi_{0n}^0(\mathbf{Q})> \equiv |\prod_n^N \psi_{0n}(\mathbf{q},\mathbf{Q})\left(\prod_k^{\text{modes}} \chi_{0n}^0(Q_k)\right)>; \left(\phi_{0n}^0(\mathbf{Q}) = \prod_k^{\text{modes}} \chi_{0n}^0(Q_k)\right), \quad (1)$$

where $\psi_{0n}(\mathbf{q},\mathbf{Q})$ and $\phi_{0n}^0(\mathbf{Q})$ are respectively the nth site ground electronic states and the vibrational ground states. We symbolize the collective electronic and nuclear coordinates by $\mathbf{q}$ and $\mathbf{Q}$, respectively. The suffices $0n$ of the nth-site electronic ground state denote the potential surface which determines its vibrational states. Then, we construct such a v_kth locally excited vibronic state at an mth site as

$$|e_0v_{0m}^{v_k}> \equiv |\psi_{0m}(\mathbf{q},\mathbf{Q})\phi_{0m}^{v_k}(\mathbf{Q})\prod_{n\neq m}^N \psi_{0n}(\mathbf{q},\mathbf{Q})\phi_{0n}^0(\mathbf{Q})> = |\left(\psi_{0m}(\mathbf{q},\mathbf{Q})\chi_{0m}^{v_k}(Q_k)\prod_{j\neq k}^{\text{modes}} \chi_{0m}^0(Q_j)\right) \times \left(\prod_{n\neq m}^N \psi_{0n}(\mathbf{q},\mathbf{Q})\phi_{0n}^0(\mathbf{Q})\right)>;$$

$$\left(\phi_{0m}^{v_k}(\mathbf{Q}) = \chi_{0m}^{v_k}(Q_k)\prod_{j\neq k}^{\text{mode}} \chi_{0m}^0(Q_j)\right). \quad (2)$$

By $\chi_{0n}^0(Q_k)$ and $\chi_{0n}^{v_k}(Q_k)$, we denote the vibrational ground and the v_kth excited state of the kth mode, respectively. The harmonic-oscillator model is assumed for vibrational wavefunctions. In terms of zero-order vibrationally excited states, we expand the Lth level of the total vibronically excited state of the polymer as

$$|e_0v_0^L> = \sum_m^{\text{sites}}\sum_{v_k\in m}^{\text{levels}} C_{v_km}^{(L)}|e_0v_{0m}^{v_k}> = \sum_m^{\text{sites}}\sum_{v_k\in m}^{\text{levels}} <e_0v_{0m}^{v_k}|e_0v_0^L>|e_0v_{0m}^{v_k}>, \left(\sum_m\sum_{v_k}|e_0v_{0m}^{v_k}><e_0v_{0m}^{v_k}| = 1\right). \quad (3)$$

To say nothing of including a single-state interband excitonic mixings, as in the ECO approximation,[10,11] Eq. 3 can involve a multistate interband excitonic mixing effect, arbitrarily depending upon any model which one may construct within the present theoretical framework.

The model Hamiltonian is then assumed to be

$$H = \sum_{v_k}^{\text{levels}}\sum_m^{\text{sites}} hcv_k\tilde{\nu}_{km}|e_0v_{0m}^{v_k}><e_0v_{0m}^{v_k}| + \sum_{m>n}^{\text{sites}}\sum_{v_k}^{\text{levels}}\sum_{v_l}|e_0v_{0m}^{v_k}>V_{mn}^{v_kv_l}<e_0v_{0n}^{v_l}| \equiv H_0 + V, \quad \left(E_{km}^{v_k} = \left(v_k+\frac{1}{2}\right)hc\tilde{\nu}_{km}\right), \quad (4)$$

where the first diagonal term is the sum of *bra* and *ket* operators for creating and annihilating vibronically excited levels of $\tilde{\nu}_{km}$ at site m. The second term is the sum of *bra* and *ket* interaction operators for creating vibronically excited states at site m and then transferably annihilating different vibronically excited levels at site n, or vice versa. The inter(sub)molecular interaction between the mth and nth locally excited vibronic states may be expanded about *two common points* (m and n) as

$$\begin{aligned} V_{mn}^{v_kv_l} &= <e_0v_{0m}^{v_k}|\sum_{s\in m,t\in n}^{\text{charges}}\frac{e_se_t}{r_{st}}|e_0v_{0n}^{v_l}> \\ &\approx <e_0v_{0m}^{v_k}|\boldsymbol{\mu}_m\cdot\left(\frac{|\boldsymbol{R}_{mn}|^2\mathbf{1}-3\boldsymbol{R}_{mn}\boldsymbol{R}_{mn}}{|\boldsymbol{R}_{mn}|^5}\right)\cdot\boldsymbol{\mu}_n|e_0v_{0n}^{v_l}> \\ &\equiv <e_0v_{0m}^{v_k}|\boldsymbol{\mu}_m\cdot\boldsymbol{U}_{mn}\cdot\boldsymbol{\mu}_n|e_0v_{0n}^{v_l}> \\ &= <\psi_{01}\phi_{01}^0\psi_{02}\phi_{02}^0\cdots\psi_{0m}\phi_{0m}^{v_k}\cdots\psi_{0n}\phi_{0n}^0\cdots\psi_{0N}\phi_{0N}^0|\boldsymbol{\mu}_m\cdot\boldsymbol{U}_{mn}\cdot\boldsymbol{\mu}_n \\ &\qquad |\psi_{01}\phi_{01}^0\psi_{02}\phi_{02}^0\cdots\psi_{0m}\phi_{0m}^0\cdots\psi_{0n}\phi_{0n}^{v_l}\cdots\psi_{0N}\phi_{0N}^0> \\ &= <\psi_{0m}\phi_{0m}^{v_k}|\boldsymbol{\mu}_m|\psi_{0m}\phi_{0m}^0>\cdot\boldsymbol{U}_{mn}\cdot<\psi_{0n}\phi_{0n}^0|\boldsymbol{\mu}_n|\psi_{0n}\phi_{0n}^{v_l}>, \\ &\qquad \left(\boldsymbol{\mu}_m = \sum_t^{\text{charges}} e_t\boldsymbol{r}_{mt};\ \boldsymbol{R}_{mn} = \boldsymbol{R}_n - \boldsymbol{R}_m\right), \end{aligned} \quad (5)$$

where the coulombic interaction operators of the first line are approximated by such a dipole–dipole interaction operator, $\boldsymbol{\mu}_m\cdot\boldsymbol{U}_{mn}\cdot\boldsymbol{\mu}_n$, as given in the second line. By the dipole–dipole interaction operator with respect to m and n, pickup of m,n-vibronic parts in the left

v_kth and the right v_lth excited state functions and also the orthogonality of the other state functions lead to the last line of Eq. 5. $\boldsymbol{U}_{mn}$ defines the unit dipole–dipole interaction tensor and $\boldsymbol{R}_{mn}$ is the distance vector. However, in relation to the following Eq. 11, Eq. 5 is clearly awkward when we would like to consider any multi-level interband mixings, since the transition moments of different levels are known to prefer different adequate positions, so as to obtain good agreement with the experimental bandshapes. The problem regarding this difficulty is mentioned in the final section.

Following the fixed-charge approximation,[6] we assume in Eq. 5 that the (sub)molecule can be regarded as being an aggregate of oscillating atoms of fixed charge. Therefore, the vibronic transition moment of an mth site residue may be calculated by

$$\begin{aligned}
&< \psi_{0m}\phi_{0m}^{v_k}|\boldsymbol{\mu}_m|\psi_{0m}\phi_{0m}^{0} > \\
&\quad \equiv < \psi_{0m}\phi_{0m}^{v_k}| \sum_{t}^{\text{charges}} e_t \boldsymbol{r}_{mt}|\psi_{0m}\phi_{0m}^{0} > \\
&\quad = < \psi_{0m}\phi_{0m}^{v_k}| \sum_{t}^{\text{charges}} e_t(\boldsymbol{R}_{mt}+\boldsymbol{\rho}_t)|\psi_{0m}\phi_{0m}^{0} > \\
&\quad = < \phi_{0m}^{v_k}(\mathbf{Q})| \sum_{t}^{\text{charges}} e_t \boldsymbol{R}_{mt} + \sum_{t}^{\text{charges}} e_t\boldsymbol{\rho}_t|\phi_{0m}^{0}(\mathbf{Q}) >_Q \\
&\quad \equiv \boldsymbol{\mu}_{0m}^{v_k 0},
\end{aligned} \tag{6}$$

where $\boldsymbol{r}_{mt}$ is an instantaneous position vector associated with an effective charged-particle e_t. This position vector is then resolved into the equilibrium position vector, $\boldsymbol{R}_{mt}$, of atom t, and its instantaneous displacement, $\boldsymbol{\rho}_t$, from equilibrium. The latter is expressed in terms of normal coordinates. The fourth line of Eq. 6 is obtained after integration over $\boldsymbol{q}$. The operator of the first term means the permanent dipole moment, whose integration over nuclear coordinates, however, vanishes because of the orthogonality of the vibrational wavefunctions.

Experimentally, in the Gaussian band approximation of a monomer band, a formula used to evaluate the absolute value of the transition moment can be derived from Bayley's review[18] as

$$\begin{aligned}
|\boldsymbol{\mu}_{0m}^{v_k 0}|^2 &\approx 0.98\times 10^{-38}\frac{\varepsilon_{\max}^{\text{exptl}}\tilde{\Gamma}_{v_k}^{\text{FWHH}}/2}{\tilde{\nu}_{km}} \\
&= 0.98\times 10^{-38}\frac{\varepsilon_{\max}^{\text{exptl}}\eta_{v_k}}{\tilde{\nu}_{km}}, \quad [(\text{esu cm})^2],
\end{aligned} \tag{7}$$

where 0.98 comes to be 0.92 for the Lorentzian bandshape approximation.[12,19] $\tilde{\Gamma}_{v_k}^{\text{FWHH}}$ defines the full-width of the monomer IR band at the half-peak height (FWHH) in units of wavenumbers. η_{v_k} is a damping factor related to Eq. 8 given below. The directions of the transition moments are taken from Sandeman's analysis of the amide I and II bands in N,N'-diacetylhexamethylenediamine.[20] The use of the thus-obtained model Hamiltonian is made to derive the vibrational polarizability tensors.

Vibrational Polarizability Tensor of Polymer

We are now in a position to derive the vibrational transition polarizability tensor in order to describe the VCD and IR absorption bands. From Eq. 4, a crude Green's operator for a polymer is defined as

$$\begin{aligned}
G_\circ(\tilde{\nu}) &= \frac{1}{hc\tilde{\nu}-H_\circ+i\eta} \\
&= \sum_{m}^{\text{sites}}\sum_{v_k\in m}^{\text{levels}} \frac{|e_0 v_{0m}^{v_k}><e_0 v_{0m}^{v_k}|}{hc(\tilde{\nu}-v_k\tilde{\nu}_{km}+i\eta_{v_k})},
\end{aligned} \tag{8}$$

from which we can define the vibrational transition polarizability tensors of monomers,

$$\begin{aligned}
&-<e_0v_0^0|\boldsymbol{\mu}G_\circ(\tilde{\nu})\boldsymbol{\mu}|e_0v_0^0> \\
&\quad = \sum_{m}^{\text{sites}}\left(\sum_{v_k\in m}^{\text{levels}}\frac{-\boldsymbol{\mu}_{0m}^{0v_k}\boldsymbol{\mu}_{0m}^{v_k0}}{hc(\tilde{\nu}-v_k\tilde{\nu}_{km}+i\eta_{v_k})}\right) \equiv \sum_{m}^{\text{sites}}\boldsymbol{\alpha}_{mm}^{v}(\tilde{\nu}).
\end{aligned} \tag{9}$$

In Eq. 9, $\tilde{\nu}$,$\tilde{\nu}_{km}$, and η_{v_k} are defined in units of wavenumbers and $\boldsymbol{\mu}_{0m}^{0v_k}/e$ is given in units of cm with $e^2/hc=1.161385\times10^{-3}$. Regarding the vibrational quantum number (v_k) in the present calculations, such a one-quantum transition as $0_k\rightarrow 1_k$ is only taken into account in Eqs. 8 and 9.

For a true Green's operator, we can derive the total vibrational transition polarizability tensor. By making use of the relationships

$$\begin{aligned}
&-<e_0v_0^0|\boldsymbol{\mu}G(\tilde{\nu})\boldsymbol{\mu}|e_0v_0^0> \\
&=-<e_0v_0^0|\boldsymbol{\mu}(hc\tilde{\nu}-H+i\eta)^{-1}\boldsymbol{\mu}|e_0v_0^0> \\
&\equiv \sum_{m}^{\text{sites}}\sum_{n}^{\text{sites}} {}^{p}\boldsymbol{\alpha}_{mn}^{v}(\tilde{\nu}) \\
&=-<e_0v_0^0|\boldsymbol{\mu}\{G_\circ(\tilde{\nu})+G_\circ(\tilde{\nu})VG_\circ(\tilde{\nu}) \\
&\qquad +G_\circ(\tilde{\nu})VG_\circ(\tilde{\nu})VG_\circ(\tilde{\nu})+\cdots\}\boldsymbol{\mu}|e_0v_0^0>,
\end{aligned} \tag{10}$$

insertion of the resolution of identity given in Eq. 3 leads to the vibrational polarizability tensor of the polymer,[15]

$$\begin{aligned}
{}^{p}\boldsymbol{\alpha}_{mn}^{v}(\tilde{\nu}) &= \boldsymbol{\alpha}_{mm}^{v}(\tilde{\nu})\delta_{mn} - \boldsymbol{\alpha}_{mm}^{v}(\tilde{\nu})\cdot\boldsymbol{U}_{mn}\cdot\boldsymbol{\alpha}_{nn}^{v}(\tilde{\nu}) \\
&\quad + \sum_{k=1}^{N}\boldsymbol{\alpha}_{mm}^{v}(\tilde{\nu})\cdot\boldsymbol{U}_{mk}\cdot\boldsymbol{\alpha}_{kk}^{v}(\tilde{\nu})\cdot\boldsymbol{U}_{kn}\cdot\boldsymbol{\alpha}_{nn}^{v}(\tilde{\nu}) - \cdots \\
&= [1+\boldsymbol{\alpha}^{v}(\tilde{\nu})\cdot\mathsf{U}]_{mn}^{-1}\cdot\boldsymbol{\alpha}_{nn}^{v}(\tilde{\nu}), \\
&\qquad (m,n=1,2,3,\cdots,N),
\end{aligned} \tag{11}$$

where the sans serif type represent $3N\times3N$ matrices.

Following theoretical treatments of the electronic CD made by Applequist[21] and ours,[15] we can thus derive the molar ellipticity of VCD per residue as

$$\begin{aligned}
&[\theta(\tilde{\nu})] = 288\pi^2 N_A\tilde{\nu}^2\frac{1}{N}\sum_{m=1}^{N}\sum_{n=1}^{N} Im\{\frac{1}{12}\boldsymbol{R}_{mn}\cdot{}^{p}\boldsymbol{\alpha}_{mn}^{v}(\tilde{\nu}) : \boldsymbol{\varepsilon}\}, \\
&\qquad (\text{deg cm}^2\,\text{dmole}^{-1}),
\end{aligned} \tag{12a}$$

where we follow the tensor notation of Applequist,[21] and $\boldsymbol{R}_{mn}$ is defined in units of cm, N_A being Avogadro's number. After obtaining the left-hand side of Eq. 11, calculations of Eq. 12a are performed by

$$\begin{aligned}
&\boldsymbol{R}_{mn}\cdot{}^{p}\boldsymbol{\alpha}^{v}_{mn}(\tilde{\nu}):\boldsymbol{\varepsilon}\\
&\quad=\sum_{i}^{(x,y,z)}\sum_{j}\sum_{k}(R_{mn})_i\varepsilon_{ijk}\,{}^{p}\alpha^{v,kj}_{mn}(\tilde{\nu})\\
&\quad=\sum_{i}^{(x,y,z)}\sum_{j}\sum_{k}(R_{mn})_i\,{}^{p}\alpha^{v,jk}_{mn}(\tilde{\nu})\varepsilon_{kji}\\
&\quad=x_{mn}\{{}^{p}\alpha^{v,zy}_{mn}(\tilde{\nu})-{}^{p}\alpha^{v,yz}_{mn}(\tilde{\nu})\}\\
&\qquad+y_{mn}\{{}^{p}\alpha^{v,xz}_{mn}(\tilde{\nu})-{}^{p}\alpha^{v,zx}_{mn}(\tilde{\nu})\}\\
&\qquad+z_{mn}\{{}^{p}\alpha^{v,yx}_{mn}(\tilde{\nu})-{}^{p}\alpha^{v,xy}_{mn}(\tilde{\nu})\}. \qquad (12b)
\end{aligned}$$

Here ε_{ijk} is the Levi–Civita symbol. Correspondingly, we obtain the bandshape function of the vibrational absorption per residue, i.e., the molar extinction coefficient as follows:

$${}^{p}\varepsilon(\tilde{\nu})=(8\pi^2N_{\mathrm{A}}/2302.6)\tilde{\nu}\frac{1}{N}\sum_{m}^{N}\sum_{n}^{N}Im[\frac{1}{3}Tr\ {}^{p}\boldsymbol{\alpha}^{v}_{mn}(\tilde{\nu})],$$
$$(\mathrm{dm^3\,mol^{-1}\,cm^{-1}}). \qquad (13)$$

Here, *Tr* means to take the traces of 3×3 block matrices of the $3N\times3N$ polymer polarizability tensor matrix. After all, bandshape calculations for Eqs. 12b and 13 are carried out by the point-by-point matrix inversion of Eq. 11 against the wavenumbers ($\tilde{\nu}$). Here, let us consider the relation of the present scheme with Refs. 5, 6, 7, 10, and 11. In the first-order approximation of Eq. 11 with respect to interaction potentials $\boldsymbol{U}_{mn}$ which is related with Eq. 5, Eq. 12b is derived to be

$$\begin{aligned}
&\boldsymbol{R}_{mn}\cdot{}^{p}\boldsymbol{\alpha}^{v}_{mn}(\tilde{\nu}):\boldsymbol{\varepsilon}\\
&\quad\approx\sum_{v_k\in m}^{\text{levels}}\sum_{v_l\in n}^{\text{levels}}\frac{-V^{v_kv_l}_{mn}\boldsymbol{R}_{mn}\cdot\boldsymbol{\mu}^{0v_k}_{0m}\boldsymbol{\mu}^{v_l0}_{0n}:\boldsymbol{\varepsilon}}{(hc)^2(\tilde{\nu}-v_k\tilde{\nu}_{km}+i\eta_{v_k})(\tilde{\nu}-v_l\tilde{\nu}_{ln}+i\eta_{v_l})}\\
&\quad=\sum_{v_k\in m}^{\text{levels}}\sum_{v_l\in n}^{\text{levels}}\frac{+V^{v_kv_l}_{mn}\boldsymbol{R}_{mn}\cdot\boldsymbol{\mu}^{0v_k}_{0m}\times\boldsymbol{\mu}^{v_l0}_{0n}}{(hc)^2(\tilde{\nu}-v_k\tilde{\nu}_{km}+i\eta_{v_k})(\tilde{\nu}-v_l\tilde{\nu}_{ln}+i\eta_{v_l})},
\end{aligned} \qquad (14)$$

which demonstrates the familiar similarity found in the secular matrix equation methods.[5—7,10,11] Consequently, Eq. 12a involves such various interactions as those given in Eq. 5 up to infinite-order terms.

By making use of the rotation matrix $\boldsymbol{R}(\phi,\psi)$, which Pysh[22,23] derived by following the method of Ooi et al.,[24] we can construct the geometries of polypeptides (*N*-mers) with repeating chromophore units, such as $-[C_\alpha R(H)-(C'O)-NH]_n-$, by putting the *x*,*y*-plane on the first amide plane (C′ONH). The chosen polymer coordinate system enables us to directly use monomer spectroscopic data, such as the electric and magnetic transition moments, without any transformation, since we describe the *x*,*y*,*z*-components of these moments in terms of the Cartesian coordinates assumed on the first C′ONH-plane for the polymer coordinate system. A more concrete algorithm is mentioned in the following.

Here, by using $\boldsymbol{r}_n$, we represent each atomic position vector belonging to the *n*th residue. Also by using $\boldsymbol{\mu}_n$, we represent each vibrationally induced electric moment belonging to the same *n*th residue. They can then be successively computed from the position vector and the moment vector belonging to the preceeding $(n-1)$th residue, starting from the position vector and the moment vector of the first site, $\boldsymbol{r}_1$ and $\boldsymbol{\mu}_1$, as follows:

$$\begin{aligned}
&\boldsymbol{r}_n=\boldsymbol{R}(\phi,\psi)\boldsymbol{r}_{n-1}+\boldsymbol{r}_{\text{translation}}, \quad \text{and/or}\\
&\boldsymbol{\mu}_n=\boldsymbol{R}(\phi,\psi)\boldsymbol{\mu}_{n-1}, \qquad (15)
\end{aligned}$$

where $\boldsymbol{r}_n$, $\boldsymbol{\mu}_n$, and $\boldsymbol{r}_{\text{translation}}$ are represented by column matrices. The rotation matrix $\boldsymbol{R}(\phi,\psi)$ is a function of the conventional ϕ and ψ torsion angles. These relationships and parameters are illustrated in Fig. 1. The second equation of Eq. 15 can be clearly derived from the first one, since the head and tail of a certain vector can be given by the coordinates of the amide plane to which the vector belongs. However, in the expression of Eq. 15, we make use of the transposed form of the rotation matrix given by Pysh,[22] since he has defined the position vectors in terms of row matrices. In computations, we employ his starting coordinates for the first residue, $\{\boldsymbol{r}_1\}$, together with the pitch, i.e., the *x*,*y*,*z*-components of $\boldsymbol{r}_{\text{translation}}$ (3.519−1.436, 0.0) in units of A.

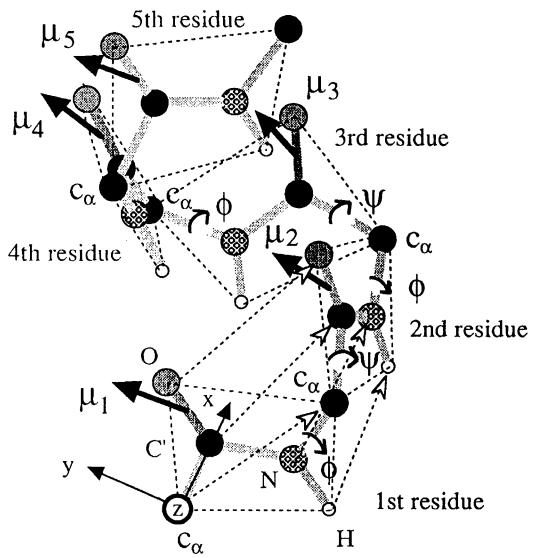

Fig. 1. Definitions of the dihedral torsion angles (ϕ,ψ) of a polypeptide backbone and positioning of the amide I transition moments of residues. The five dashed arrows from the first residue to the second one represent the rotational 3×3 matrix operations, $\boldsymbol{R}(\phi,\psi)$, of five atomic positions together with the translations, $\boldsymbol{r}_{\text{translation}}$, of the five positions.

Results and Discussion

The vibrational polymer polarizability tensor has been formulated for obtaining the VCD and IR absorption bandshapes of biopolymers. The calculations (as shown in Figs. 2, 3, 4, 5, 6, and 7) were carried out by considering only the same single-level exciton coupling for each amide I and II band, which means neglecting any interband mixing effects between different excited

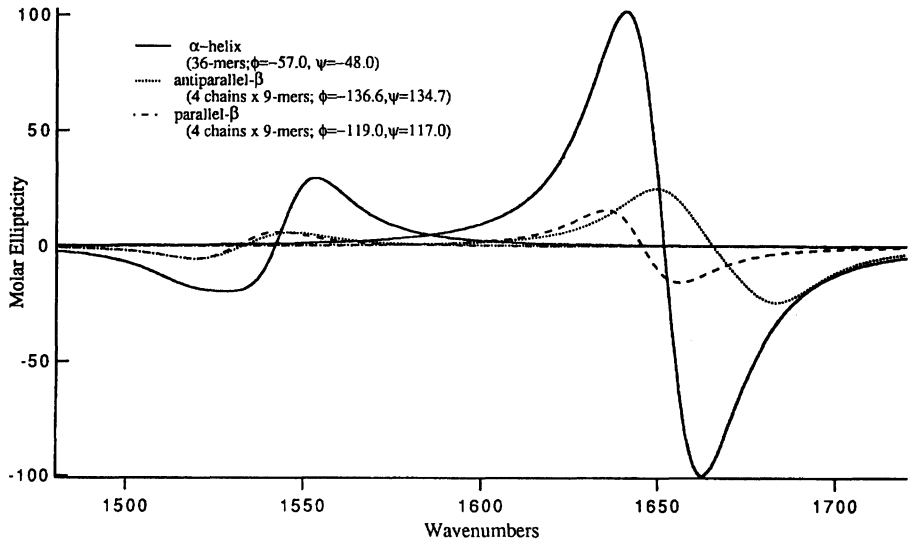

Fig. 2. Computed VCD curves of amide I and II regions for α-helical (36-mers), antiparallel β-sheet (4 chains×9-mers), and parallel β-sheet (4 chains×9-mers) polypeptides.

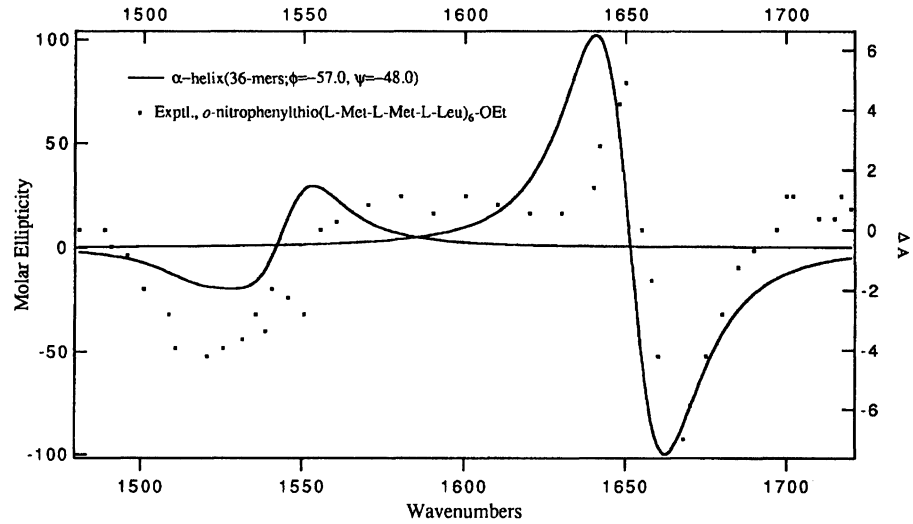

Fig. 3. Comparison of computed VCD curves of amide I and II regions for α-helical polypeptide (36-mers) with the experimental VCD curve[27] of *o*-nitrophenylthio(L-Met–L-Met–L-Leu)$_6$–OEt, where ΔA for the right ordinate represents, in arbitrary units, the experimentally observed difference of IR absorbances between the left and right circularly polarized lights.

levels. Consequently, these calculations come to be essentially the same as the excitonic treatments for the secular matrix equation method of Snir et al.[7] as well as the ECO approximation.[10—14] However, the two-level interband mixings are taken into account in Fig. 8.

Throughout the present calculations, we made use of the experimental data of the amide I band peaked at 1650 cm^{-1} and the amide band II peaked at 1550 cm^{-1}.[20] The transition moment of amide I, 0.29D, is inclined at an angle 19° from the C′O bond towards the C′O$_\alpha$ bond, and the transition moment of amide II, 0.22D, at an angle of 68° from the C′O bond towards the C′C$_\alpha$ bond. The damping factors (η_I and η_{II}) were taken to be 17 cm^{-1}. In separate calculations for the amide I and II bands from one another, we put the two different transition moments at different positions in each residue, one being positioned at 0.4 *C′=O bond length from the oxygeon atom, and the other at a 0.5*NH bond length.[7]

In Fig. 2, the computed VCD bandshapes for α-helical and β-sheet polypeptides are given. We compare the computed VCD and IR absorption bands of α-helix with the experimental bands[27] in Figs. 3 and 4. As shown in Figs. 2, 3, and 4, the VCD and IR absorption bandshapes computed for α-helical and β-sheet polypeptides gave qualitatively similar results compared with those bandshapes computed by Snir et al.[7] While the present calculations make use of the dipole–dipole potentials, based upon experimental data concerning the transition moments, the calculations of Snir et al.[7] made use of empirical potentials determined by the IR data of Miyazawa and Blout.[25] In the amide II region of the

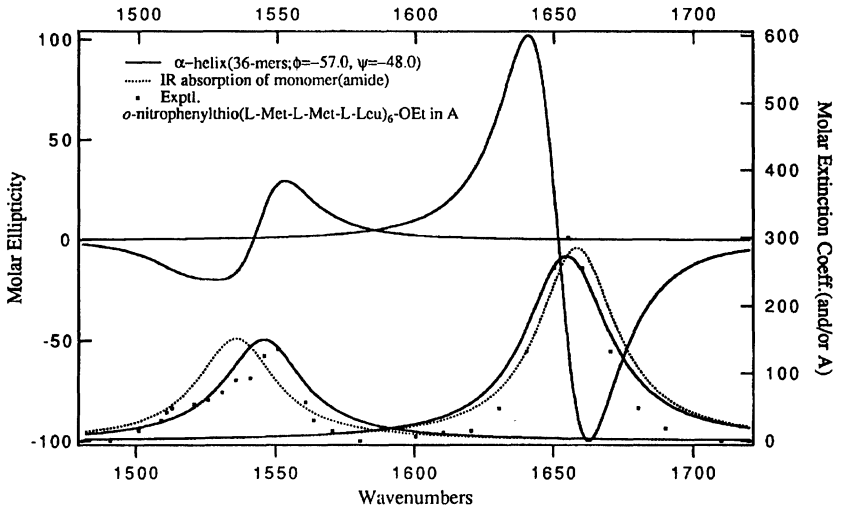

Fig. 4. Comparison of computed IR absorption curves of amide I and II regions for α-helical polypeptide (36-mers) with the experimental IR absorption curves of amide I and II for o-nitrophenylthio (L-Met–L-Met–L-Leu)$_6$–OEt[27] and correspondingly computed VCD curve of α-helical (36-mers), where A for the right ordinate represents the experimentally observed IR absorbance in arbitrary units.

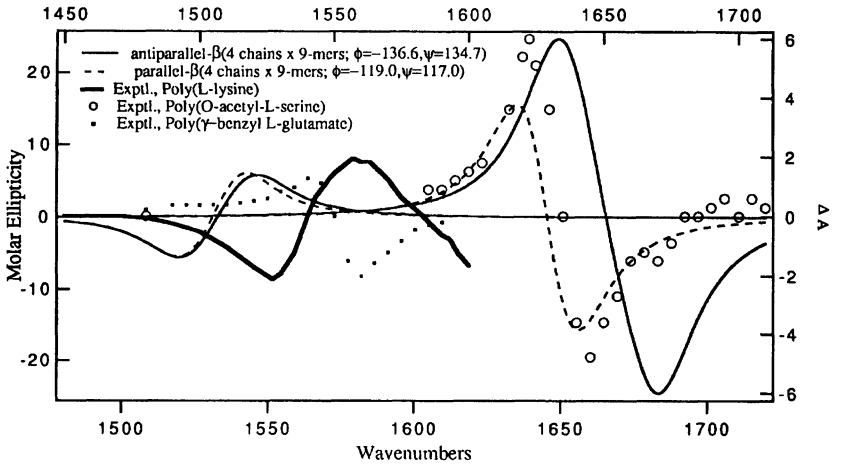

Fig. 5. Comparison of computed VCD curves of amide I and II regions for antiparallel β-sheet (4 chains×9-mers), and parallel β-sheet (4 chains×9-mers) polypeptides with experimental VCD curves of poly(L-lysine)[28] and poly(O-acetyl-L-serine) and poly(γ-benzyl L-glutamate),[29] where ΔA for the right ordinate represents the experimentally observed difference of IR absorbances between the left and right circularly polarized lights in arbitrary units.

α-helix conformations, the calculations by Snir et al.[7] for the coupling parameters of Miyazawa and Blout[25] gave different VCD profiles with a sign reversal from their own results obtained by making use of the parameters of Krimm.[26] Their calculations for the former parameters[25] are found to coincide with present calculations.

Figures 5, 6, and 7 compare the VCD and IR bands for antiparallel and parallel β-sheet polypeptides with the experimental VCD and IR bands.[29] In the amide II region of antiparallel β-sheet structures as (shown in Fig. 5), it is revealed that not only our CD calculations with the dipole–dipole interaction potentials, but also the CD calculations of Snir et al.[7] with the IR empirical potentials predict the experimentally observed negative–positive bisignate curve viewed from low wavenumbers.[28] Such an observed bisignate VCD curve, however, is found to be at the higher side of wavenumbers shifted from the computed curve, whereas the observation sometime gives a positive-negative bisignate curve.[29] In relation to this, this discrepancy in the model calculations demands us to rescrutinize the parameters of monomer transition moments as well as the molecular structures represented by the polypeptide backbone torsion angles (ϕ,ψ). We must also consider any changes in the transition moments due to a side-chain effect in our calculation scheme. Figures 6 and 7 compare the correspondingly computed IR absorption bands with the experimental ones,[29] which require considerations of any disagreements in the IR absorption bandshift as well as the VCD bandshifts of Fig. 5 in future work.

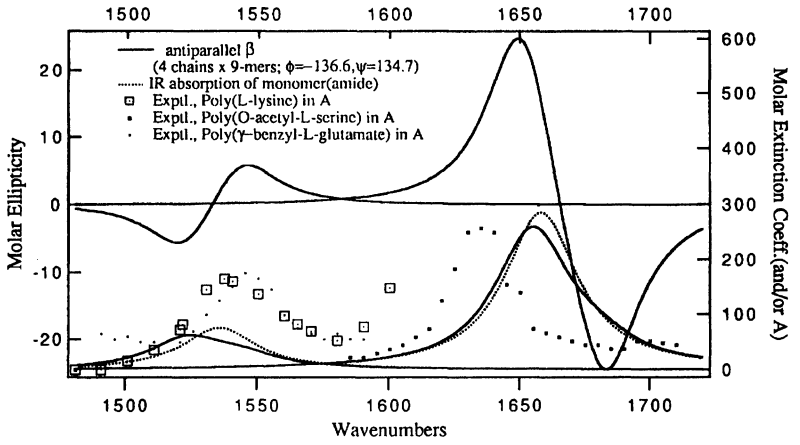

Fig. 6. Comparison of computed IR absorption curves of amide I and II regions for antiparallel β-sheet (4 chains×9-mers) polypeptides with experimental IR absorption curves of poly(L-lysine)[28] and poly(*O*-acetyl-L-serine) and poly(γ-benzyl L-glutamate)[29] and correspondingly computed VCD curves, where A for the right ordinate represents the experimentally observed IR absorbance in arbitrary units.

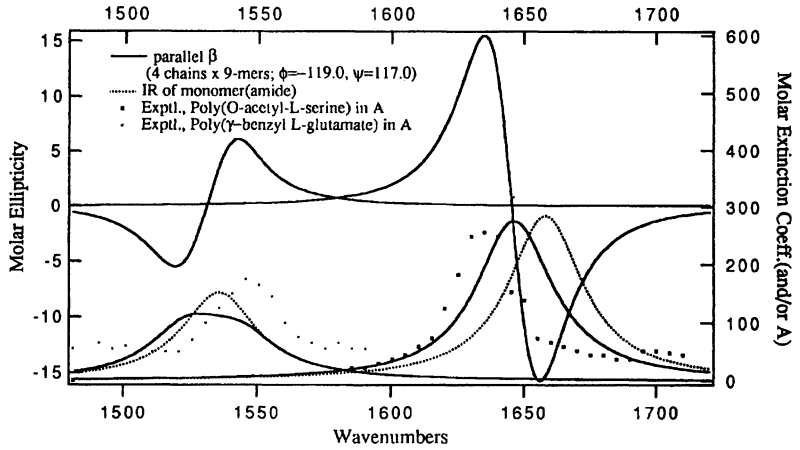

Fig. 7. Comparison of computed IR absorption curves of amide I and II regions for parallel β-sheet (4 chains×9-mers) polypeptides with experimental IR absorption curves of poly(*O*-acetyl-L-serine) and poly(γ-benzyl L-glutamate)[29] and correspondingly computed VCD curves, where A for the right ordinate represents the experimentally observed IR absorbance in arbitrary units.

Equation 11, derived from Eq. 3, can involve any *interband mixings* between different vibrational modes. However, when we take into account the interband mixings in Eq. 11, there is such a limitation that different transition moments within a residue must be located at the same common places on account of the definition of Eq. 5. For such cases in which we like to position different transition moments of each residue at different positions within each residue, we must require a reinterpretation of Eq. 11, as is mentioned below. Alternatively, we must develop a more sophisticated formalism, which will be presented elsewhere. In Fig. 8, the different level interband mixings of the amide I and II bands between monomers were taken into account. If we take different numberings for all of the monomer transition moments in order to put the different transition moments of certain residues onto different positions within the residues, and if we do not take into account intra(sub)molecular interactions, the present formalism can then be safely used. Thus, as shown in Fig. 8, although the two-state interband mixing effects give noticeably different bandshapes, there are no changes in their qualitative features. For instance, the bisignate VCD amide II band computed for α-helix comes to be a skewed bisignate type, which is considered to be a result of intensity borrowing due to the two-state interband mixings. It appears possible to expect that we can predict the experimentally observed monosignate band through multistate interband mixings if we properly choose the parameters involving the structural factors in relation to inter(sub)molecular interactions. For a certain case, the interband interactions may become more serious than the results given in Fig. 8 indicate.

The present VCD formalism excludes any asymmetric effect of a residue, such as intrinsic optical activity or the asymmetrically induced couplings of magnetic transition moments with the vibrationally induced transition moments through dipole–dipole interactions.

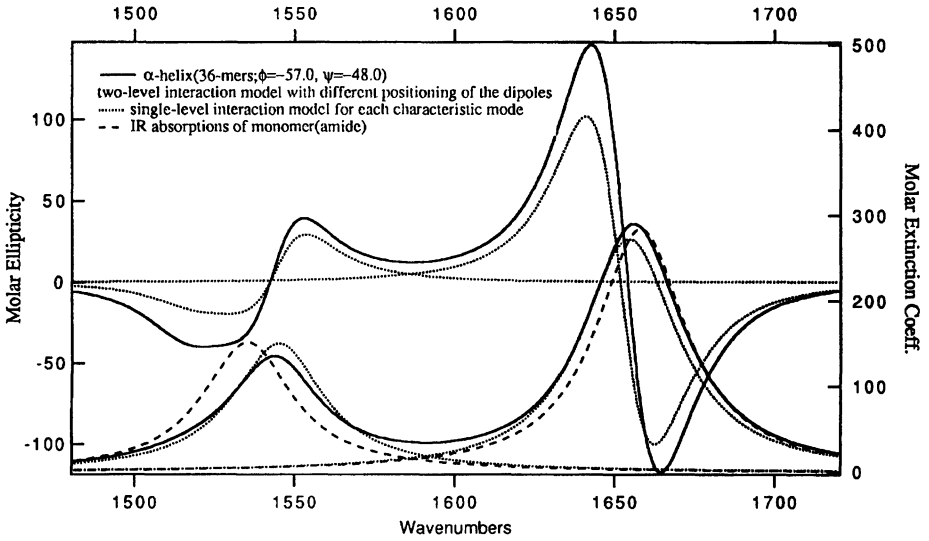

Fig. 8. Computed VCD curves in amide I and II regions for α-helical (36-mers) by allowing for two-state interband mixings.

Furthermore, it is difficult to obtain information concerning these magnetic moments, the importance of which is generally recognized.[3,7,30] If we can establish how to estimate the vibrationally induced magnetic moments correctly, and/or if the correct vibrationally induced magnetic moments are experimentally available, the present theory may be extended to involve intrinsic asymmetric effects of residues by following a similar treatment of electronic CD theory.[31]

References

1) T. A. Keiderling, *Nature*, **322**, 851 (1986).
2) S. C. Yasui and T. A. Keiderling, *J. Am. Chem. Soc.*, **108**, 5576 (1986).
3) M. G. Paterlini, T. B. Freedman, and L. A. Nafie, *Biopolymers*, **25**, 1751 (1986).
4) S. C. Yasui and T. A. Keiderling, *Biopolymers*, **25**, 5 (1986).
5) G. Holtzwarth and I. Chabay, *J. Chem. Phys.*, **57**, 1632 (1972).
6) J. A. Schellman, *J. Chem. Phys.*, **58**, 2882 (1973).
7) J. Snir, R. A. Frankel, and J. A. Schellman, *Biopolymers*, **14**, 173 (1975).
8) Yu. N. Chirgadze and N. A. Nevskaya, *Biopolymers*, **15**, 607 (1976).
9) Yu. N. Chirgadze and N. A. Nevskaya, *Biopolymers*, **15**, 627 (1976).
10) M. Gulotta, D. J. Goss, and M. Diem, *Biopolymers*, **28**, 2047 (1989).
11) W. Zhong, M. Gulotta, D. J. Goss, and M. Diem, *Biochemistry*, **29**, 7485 (1990).
12) O. Lee, G. M. Roberts, and M. Diem, *Biopolymers*, **28**, 1759 (1989).
13) H. R. Wyssbrod and M. Diem, *Biopolymers*, **32**, 1237 (1992).
14) S. S. Birke, I. Agbaje, and M. Diem, *Biochemistry*, **31**, 450 (1992).
15) H. Ito and Y. J. I'Haya, *J. Chem. Phys.*, **77**, 6270 (1982).
16) D. P. Craig and T. Thirunamachandran, *Mol. Phys.*, **35**, 825 (1978).
17) C. J. Barnett, A. F. Drake, R. Kuroda, and S. F. Mason, *Mol. Phys.*, **41**, 455 (1980).
18) P. M. Bayley, *Prog. Biophys. Mol. Biol.*, **27**, 1 (1973).
19) J. B. Birks, "Photophysics of Aromatic Molecules," Wiley-Interscience, London (1970), p. 51.
20) I. Sandeman, *Proc. R. Soc., London, Ser. A*, **232**, 105 (1955).
21) J. Applequist, *J. Chem. Phys.*, **58**, 4251 (1973).
22) E. S. Pysh, *J. Chem. Phys.*, **52**, 4723 (1970).
23) D. Aebersold and E. S. Pysh, *J. Chem. Phys.*, **53**, 2156 (1970).
24) T. Ooi, R. A. Scott, G. Vanderkooi, and H. A. Scheraga, *J. Chem. Phys.*, **46**, 4410 (1967).
25) T. Miyazawa and E. R. Blout, *J. Am. Chem. Soc.*, **83**, 712 (1961).
26) S. Krimm, *J. Mol. Biol.*, **4**, 528 (1961).
27) S. C. Yasui, T. A. Keiderling, and R. Katakai, *Biopolymers*, **26**, 1407 (1987).
28) V. P. Gupta and T. A. Keiderling, *Biopolymers*, **32**, 239 (1992).
29) A. C. Sen and T. A. Keiderling, *Biopolymers*, **23**, 1533 (1984).
30) T. R. Faulkner, A. Moscowitz, G. Holtzwarth, E. C. Hsu, and H. S. Mosher, *J. Am. Chem. Soc.*, **96**, 252 (1974).
31) H. Ito and Y. J. I'Haya, *J. Chem. Phys.*, **98**, 8835 (1993).